Uncertainty quantification of thermo-acoustic instabilities in annular combustors

By M. Bauerheim †, A. Ndiaye ‡, P. Constantine ‖, G. Iaccarino, S. Moreau ‡‡ AND F. Nicoud ‖‖

An Uncertainty Quantification (UQ) method based on active subspace and low-order models is applied on a simplified gas turbine to determine its modal risk factor: the probability of an acoustic mode to be unstable. The configuration is a simplified 19-burner annular combustor which is operated in two different regimes, called weakly and strongly coupled regimes. Each flame is modeled by two uncertain parameters leading to a large UQ problem involving 38 parameters. The combustor is modeled as a network of 4×19 1D interconnected 1D acoustic elements which is efficiently solved quasi-analytically (ATACAMAC) as proposed recently by Bauerheim *et al.* (2014*b*). This allows us to perform a Monte Carlo analysis (approx. $10,000$ ATACAMAC calculations), assuming that the uncertainties on the inputs are known. The reference Monte Carlo risk factor is then compared with that obtained by a less demanding UQ method. First, the dimension of the problem is reduced from 38 to only 3 parameters for the two regimes considered by the active subspace approach based on gradient correlations. Then, linear and quadratic analytical models based on the three active variables are fit using 100 ATACAMAC simulations. These low-order models are then replayed $100,000$ times to obtain the PDF of the growth rate as well as the risk factor estimation. Results show that for both regimes, the UQ method is able to accurately predict the risk factor of the configuration.

1. Introduction

It has long been known that combustion instabilities in industrial systems can lead to strong acoustic oscillations which arise when pressure and heat release fluctuations are in phase (Lieuwen & Yang 2005). In extreme cases these instabilities can increase the amplitude of the flame motion and/or the level of structural vibrations and eventually destroy part of the combustor. Consequently, there is a need to better understand combustion instabilities and to be able to predict them at the design level, although the physical mechanisms involved are various and complex (Lieuwen & Yang 2005).

Several recent studies have shown that the Large Eddy Simulation (LES) approach is a powerful tool for studying the dynamics of turbulent flames and their interactions with the acoustic waves. However, these simulations are very CPU demanding and faster tools are required in the design process of new burners. A natural approach is to characterize the stable/unstable modes in the frequency domain. An approximate linear wave equation for the small pressure perturbations $p(\vec{x},t) = \tilde{p}(\vec{x})\exp(-j\omega t)$ in reacting flows may be

† SNECMA, France
‡ CERFACS, France
‖ Colorado School of Mines, CO
‡‡ University of Sherbrooke, Canada
‖‖ University of Montpellier, France

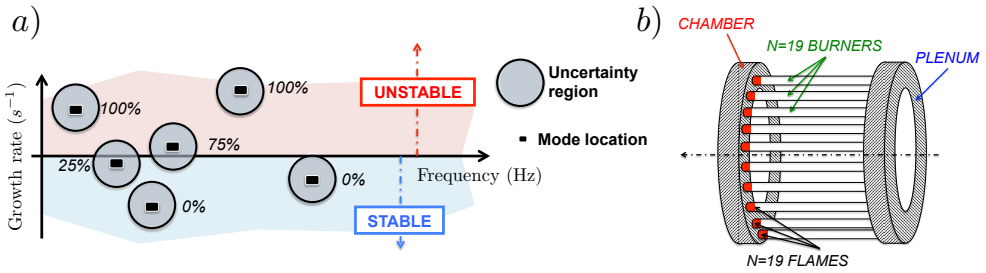

FIGURE 1. a) Location in the frequency plane of the first six thermo-acoustic modes in a typical combustor without uncertainties (single point, black symbols) and with uncertainties (each mode belongs to an admissible region of the frequency plane with an associated risk factor to be unstable). b) The annular configuration studied with one plenum connecting $N = 19$ burners and an annular chamber.

derived from the Navier-Stokes equations (Poinsot & Veynante 2005) and reads:

$$\nabla \cdot \left(c_0^2 \nabla \tilde{p}\right) + \omega^2 \tilde{p} = j\omega(\gamma - 1)\tilde{\dot{\omega}}_T, \tag{1.1}$$

where $\dot{\omega}_T(\vec{x}, t) = \widetilde{\dot{\omega}}_T(\vec{x}) \exp(-j\omega t)$ is the unsteady heat release, c_0 the speed of sound, and ω is the complex pulsation.

In order to close the problem, the flame is often modeled as a purely acoustic element thanks to an $n-\tau$ type of model (Crocco 1952) or a matrix transfer (Polifke *et al.* 2001), which essentially relates the unsteady heat release to acoustic quantities at reference locations. Eq. (1.1) then corresponds to a non-linear eigenvalue problem which can be solved efficiently at reduced cost (Nicoud *et al.* 2007). The output of such a low-order tool is typically a map of the thermo-acoustic modes in the complex plane (see the black symbols in Figure 1 (a)). In this view, each mode is either stable or unstable, depending on the input parameters of the thermacoustic analysis. Each mode corresponding to a positive imaginary frequency (positive growth rate) is linearly unstable and must be controlled (e.g., by including acoustic dampers) for the combustor to be stable. The design process is made much more complex by the fact that the input parameters of the low-order model described by Eq. (1.1), are uncertain. For example, the speed of sound c_0, the boundary impedances, and the flame forcing $\dot{\omega}_T(\vec{x}, t)$ are very sensitive to multiple physical parameters such as the flow regime, manufacturing tolerances, fuel changes, and acoustic and heat losses which are themselves (partly) unknown. As a consequence, each mode actually belongs to an uncertain region in the complex planen as illustrated in Figure 1 (a) and quantified by the risk factor, the probability for the mode to be unstable.

In simplified designs containing only one burner, the shape and size of these uncertain regions depend on only a few uncertain parameters such as the inlet air temperature, the amplitude and phase of the flame response, and the boundary impedances. The situation is more complex in actual industrial combustors as used for power generation or aero-engines: they usually contain an annular chamber hosting several burners, typically from 15 to 24, and are prone to azimuthal combustion instabilities. In this case, the number of uncertain parameters may reach several tens since the gain and time delay of each burner (and associated flame) is highly sensitive to manufacturing tolerances. The curse of dimensionality is thus becoming an issue when applying UQ to such systems. Moreover, the coupling between the combustion chamber, the burners, and the upstream plenum is also rather complex, as revealed by recent experimental (Worth

& Dawson 2013) and numerical (Wolf *et al.* 2012) studies. Recently developed analytical descriptions of the thermoacoustics of annular combustors with (Bauerheim *et al.* 2014*b*) burner heterogeneities open new perspectives regarding parametric studies and uncertainty quantification (UQ) in these complex systems. To the best of our knowledge, introducing UQ for thermoacoustics was never done before although this is a necessary step to better control the risk associated with each mode during the design process. This is the objective of this study.

2. Low-order thermoacoustic model of an annular combustor

2.1. *Mathematical framework*

Over the last decades, theoretical approaches have progressed and been adapted to simplified annular configurations (Noiray *et al.* 2011; Bauerheim *et al.* 2014*b*) to complement 3D Helmholtz simulations (Pankiewitz & Sattelmayer 2003) and LES (Wolf *et al.* 2012). Recently, the analytical-based ATACAMAC tool (Analytical Tool to Analyze and Control Azimuthal Mode in Annular Chambers) has been developed to handle more complex geometries with an arbitrary number of burners (Bauerheim *et al.* 2014*a*) or configurations with two annular cavities which can couple an annular plenum and an annular chamber (Bauerheim *et al.* 2014*b*). This study focuses on such a configuration with a 1D annular plenum which connects $N = 19$ burners and a 1D annular combustion chamber, representative of a real industrial gas turbine, as depicted in Figure 1 (b).

The ATACAMAC tool is based on the Annular Network Reduction, Figure 2 and Bauerheim *et al.* (2014*b*), which first splits the full annular combustor into N sectors containing one sector of the annular chamber and plenum and an H-connector between the annular cavities and the burners. Each sector is split into two parts:

(i) Propagation in the annular cavities (plenum or chamber): the plenum and the chamber can be treated separately. Pressure (p') and velocity (u') fluctuations in the i^{th} sector of the plenum and chamber at the azimuthal position θ, $X_\theta = [p'_p(\theta), u'_p(\theta), p'_c(\theta), u'_c(\theta)]^T$, are linked to acoustics quantities $X_{\theta+\Delta\theta}$ at the location $\theta+\Delta\theta$ by a 4-by-4 rotation matrix $R_i(\Delta\theta)$.

(ii) Interactions which couple the annular plenum and the annular chamber via the burner and the flame: acoustic pressure and velocity before the junction (θ^-) are linked to the acoustic quantities after the junction (θ^+) by a 4-by-4 matrix T_i which depends on four coupling parameters (Bauerheim *et al.* 2014*b*): $\Gamma_{i,1}$ corresponds to the plenum/burner interaction while $\Gamma_{i,4}$ is associated with the chamber/burner coupling. $\Gamma_{i,2}$ and $\Gamma_{i,3}$ are cross-interactions between the plenum and the chamber. The matrix T_i is obtained from jump conditions at null Mach number.

The 4-by-4 matrix associated with the complete i^{th} sector (interaction+propagation, which corresponds to $\Delta\theta = 2\pi/N$) is then equal to

$$X_i(\theta_0 + 2\pi/N) = R_i X_i(\theta_0^+) = R_i T_i X_i(\theta_0^-). \tag{2.1}$$

Since the quantities between neighboring sectors are equivalent ($X_i(\theta_0^-) = X_{i-1}(\theta_0 + 2\pi/N)$), using the periodicity condition ($X_{N+1}(\theta_0) = X_1(\theta_0)$) yields

$$X_1(\theta_0) = \left(\prod_{k=N}^{1} R_i T_i \right) X_1(\theta_0). \tag{2.2}$$

The eigenvector problem of Eq. (2.2) has non-trivial solutions if, and only if, its deter-

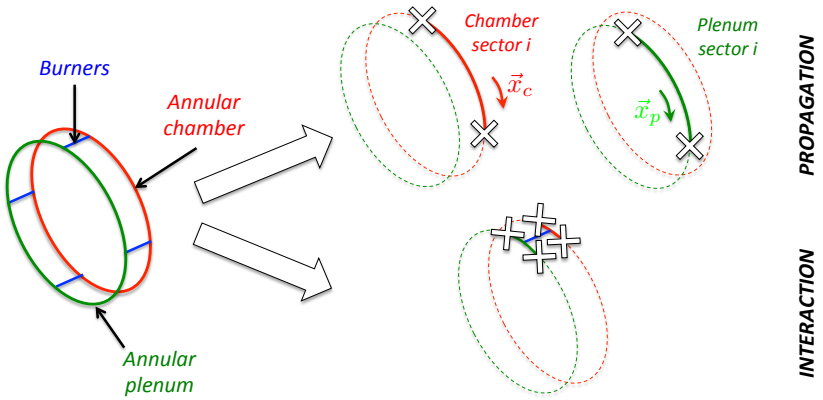

FIGURE 2. ANR methodology where the annular combustor is split into N sectors. Each sector is then split into a propagation part (top) either in the annular plenum or chamber and an interaction part (bottom between annular cavities and burners. Unknown at white cross locations are the acoustic pressure and velocity.

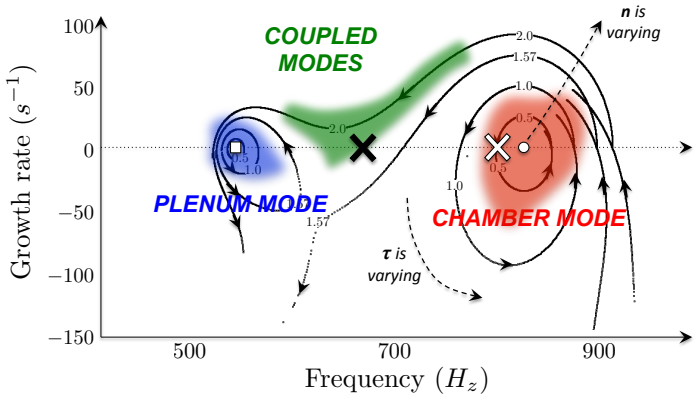

FIGURE 3. Frequencies and growth rates of modes computed using Eq. (2.3) for identical flames with FTF inputs: $n = 0.5$, 1.0, 1.57, and 2.0 ; $\tau = 0$ ms to 0.55 ms. Plenum (□) and chamber (○) modes with passive flames are also displayed. Two operating points are chosen for UQ which correspond to marginally stable weakly (white cross) or strongly (black cross) chamber modes.

minant is null leading to the dispersion relation

$$\det\left(\prod_{k=N}^{1} R_i T_i - I_d\right) = 0. \tag{2.3}$$

2.2. *Stability map*

First, the annular configuration is studied with identical burners and flames so that all coupling parameters Γ_i and matrices R_i or T_i are the same (the subscript i can be omitted in this section). Parameters of the FTF (n and τ) are varied to produce stability maps of the configuration and to unveil mode trajectories as well as coupling between cavities (Bauerheim *et al.* 2014*b*). Results are displayed in Figure 3, which highlights three different mode types: a weakly coupled chamber mode (white cross), a weakly coupled plenum mode and a strongly coupled mode (black cross).

UQ methods developed in the following will be applied on two operating points:

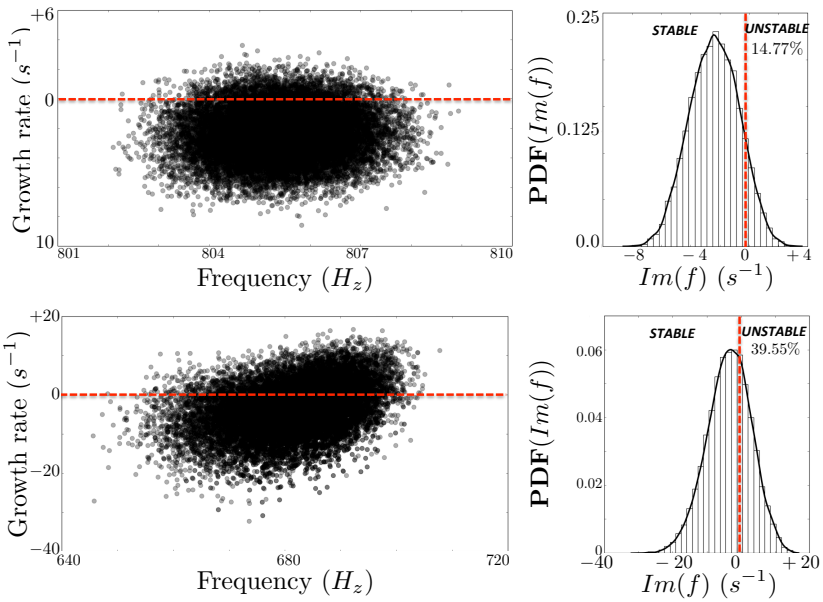

FIGURE 4. Monte-Carlo results using $M = 10,000$ samples on the weakly (top) and strongly (bottom) coupled case (left) and PDF (histogram and kernel density estimations) of the resulting growth rate (right). The risk factor is evaluated to 14.8% for the weakly coupled case and 39.5% for the strongly coupled case.

(i) Weakly coupled chamber mode with mean parameters over the $N = 19$ flames $\bar{n} = 0.5$ and $\bar{\tau} = 0.635\ ms$ and standard deviations $\sigma_n = 10\%\ \bar{n}$ and $\sigma_\tau = 5\%\bar{\tau}$.

(ii) Strongly coupled mode with mean parameters over the $N = 19$ flames $\bar{n} = 1.75$ and $\bar{\tau} = 0.735\ ms$ and standard deviations $\sigma_n = 10\%\ \bar{n}$ and $\sigma_\tau = 5\%\ \bar{\tau}$.

3. UQ analysis

3.1. *Monte Carlo analysis*

First, a Monte Carlo analysis on the full parameter space (different flames with 38 dimensions, uniform distributions) is performed on the two operating points to evaluate the risk factors. Convergence tests have proved that $10,000$ samples are sufficient to evaluate this factor as well as mean and standard deviation of the growth rate. For both the weakly (Figure 4, top) and strongly (Figure 4, bottom) coupled cases the mean growth is negative (weakly: $-2.36\ s^{-1}$; strongly: $-3.53\ s^{-1}$), meaning that the mode would be stable if predicted by standard methods. However, uncertainties on flames led to large standard deviations (weakly: $1.68\ s^{-1}$; strongly: $6.49\ s^{-1}$) so the mode can become unstable. The risk factor defined as the probability that the mode is unstable is 14.8% in the weakly coupled case and 39.5% in the strongly coupled case. Note that the strongly coupled regime leads to very high growth rate variations compared with the weakly coupled regime ($\sigma_{strongly} \sim 4\sigma_{weakly}$).

3.2. *Active subspace*

To avoid expensive Monte Carlo methods, a UQ approach called "active subspace" (Constantine *et al.* 2014) is used to reduce the dimension of the parameter space from 38D to

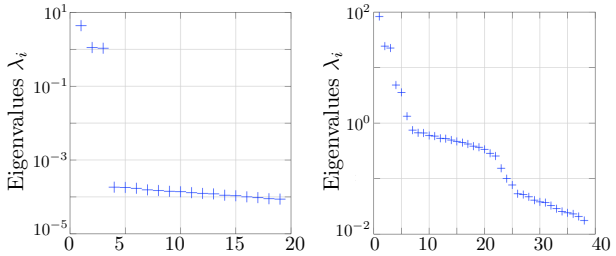

FIGURE 5. Eigenvalues λ_i for the weakly (left) and strongly (right) coupled cases using 500 samples.

just a few. First, one active subspace, based on linear regressions, is investigated showing that FTF amplitudes n_i are not significant for the weakly coupled cases: the dimension is reduced to 19 parameters for the weakly coupled case but not for the strongly coupled case. Then, to find other active variables, the method requires gradient evaluation to detect which directions in the parameter space lead to strong variations of the growth rate. Other directions leading to a flat response surface are not useful for describing the combustor stability and hence can be disregarded.

The gradient of the growth rate $g(p^k)$ with respect to the input parameters $p^k = \{n_i, \tau_i\}_{i=1..N}$ of the k^{th} sample, denoted $\nabla g(p^k) = \nabla_p^k g$, was thus computed by finite differences. The uncentered covariance matrix $\mathcal{C}$ of the gradient vector can then be expressed as

$$\mathcal{C} = \mathbf{E}[(\nabla_p^k g)(\nabla_p^k g)^T] \simeq \frac{1}{M}\sum_{k=1}^{M}(\nabla_p^k g)(\nabla_p^k g)^T, \tag{3.1}$$

where $\mathbf{E}[.]$ is the expectation operator and M is the number of samples. Since this matrix is symmetric, positive, and semidefinite, it admits a real eigenvalue decomposition:

$$\mathcal{C} = W\Lambda W^T, \quad \Lambda = \mathrm{diag}(\lambda_1, ..., \lambda_m), \quad \lambda_1 \geq ... \geq \lambda_m \geq 0, \tag{3.2}$$

where W is the eigenvector corresponding to the coefficients of a linear combination of input parameters ($W^T p$) and Λ are the eigenvalues which quantify the effect of the active variable $W^T p$ on the growth rate response $g(p)$: the higher λ_i is, the more significant the active variable $W_i^T p$ is on the average output response.

Figure 5 displays the spectrum Λ for both the weakly (left, 19 remaining directions) and the strongly (right, 38 dimensions) coupled cases. It shows that a 3D active subspace exists for the weakly coupled case and a 5D active subspace for the strongly coupled case. For the latter case, the dimension of the active subspace is less clear, which highlights the more complex physics involved in this regime where both the annular plenum and chamber act on acoustics. Eigenvalues displayed in Figure 5 converge quickly, and only 10 samples are required to identify a 3D active subspace in the weakly coupled case. However, associated eigenvectors, corresponding to linear combinations of the input parameters, have a slower convergence and require 100 samples.

The first active variable is a constant corresponding to an equi-weighted linear combination, i.e., associated with the mean flame transfer function over the $N = 19$ burners. However, the two other eigenvectors have more complex behaviors which need to be unraveled. Recent theoretical studies (Noiray *et al.* 2011; Bauerheim *et al.* 2014*a*) have shown that an annular configuration (with no plenum) is characterized by two parameters: (1) the coupling strength Σ_0 associated with the mean flame over the N burners

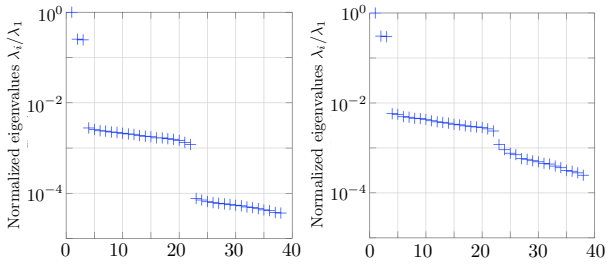

FIGURE 6. Normalized eigenvalues λ_i/λ_0 for the weakly (left) and strongly (right) coupled cases using 500 samples.

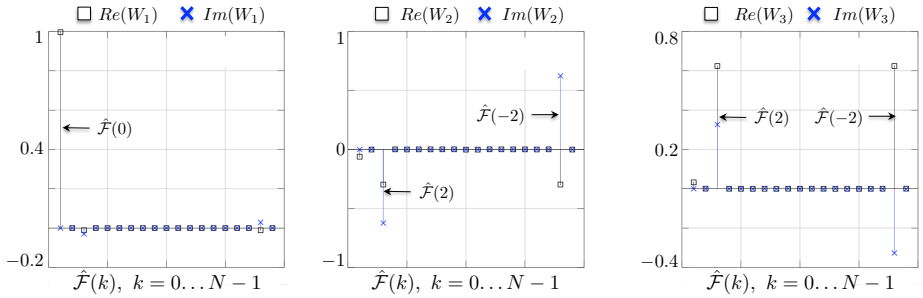

FIGURE 7. real (square) and imaginary (cross) parts of the three first active variables W_i obtained by the active subspace approach combined with a change of variable defined by Eq. (3.3) for the weakly coupled case with 1000 samples.

and (2) a splitting strength $\mathcal{S}_0$ which involves two coefficients of the Fourier transform $\widehat{\mathcal{F}}(\omega)$ of the collection of flame transfer functions $\{\mathcal{F}_i\}_{i=1..N}$: $\widehat{\mathcal{F}}(2p)$ and $\widehat{\mathcal{F}}(-2p)$, where p is the azimuthal mode order ($p = 1$ here). Note that the mean flame and therefore the coupling strength are linked to the 0^{th} coefficient of the Fourier transform: $\widehat{\mathcal{F}}(0)$.

These theoretical findings suggest that a change of variables could be used to ease the physical interpretation of active variables as well as improve the accuracy of the singular value decomposition

$$\{n_i,\ \tau_i\} \Rightarrow \{Re(\widehat{\mathcal{F}}(\omega^0)),\ Im(\widehat{\mathcal{F}}(\omega^0))\}, \tag{3.3}$$

where $\mathcal{F} = [\mathcal{F}_1, ..., \mathcal{F}_N]^T$ is the array of FTF of all the N burners viewed as a periodic complex signal, $\mathcal{F}_i(\omega^0)$ is the FTF of the i^{th} flame depending on the parameter n_i, τ_i, and the pulsation of the chamber in the absence of burners $\omega^0 = \frac{\pi c^0}{L_c}$.

Results for both the weakly (left) and strongly (right) coupled cases are displayed in Figure 6. A major difference between $\{n_i,\ \tau_i\}$ and $\{Re(\widehat{\mathcal{F}}(\omega^0)),\ Im(\widehat{\mathcal{F}}(\omega^0))\}$ formalisms is observed for the strongly coupled case, which is reduced to a 3D active subspace instead of 5D when using $n - \tau$ variables. Associated active variables shown in Figure 7 demonstrate that the effect dominating the growth rate response corresponds to the coupling strength and splitting strength involving the 0^{th} and $\pm 2^{th}$ Fourier coefficients of the flame transfer function distribution (Figure 3), as suggested by the theoretical results of Noiray *et al.* (2011) and Bauerheim *et al.* (2014*a*). Other coefficients play only a minor role, especially for the weakly coupled regime.

Models	Weakly coupled	Strongly coupled
L38	0.94	0.79
L3	0.91	0.67
Q3	0.99	0.86
AM	0.99	0.87

TABLE 1. Pearson's coefficients (Eq. (3.4)) for weakly and strongly coupled regimes using several fitting models.

Models	Weakly coupled	Strongly coupled
MC	**14.77**	**39.55**
L38	11.90	39.26
L3	11.54	34.86
Q3	14.90	41.65
AM	14.36	35.51

TABLE 2. Risk factors computed by the Monte Carlo (MC) and several fitting models (L38, L3, Q3 and AM).

3.3. *Linear regression*

The active subspace approach applied in Section 3.2 has provided successful results by reducing the 38D parameter space into a 3D space for both the weakly and strongly coupled cases involving physical quantities associated with the Fourier transform of the FTF or the $n-\tau$ parameters. A 2-step method is therefore proposed to estimate at low cost the risk factor of the first azimuthal mode: (1) a few samples are used to fit a low-order model and (2) a Monte-Carlo is applied on this low-order model. Several models with different complexities have been investigated: (i) L_{38}: a linear model based on all 38 active variables; (ii) L_3: a linear model based on the three dominant active variables; (iii) Q_3: a quadratic model (with interactions) on the three dominant active variables; (iv) AM: a linear model based on the coupling and splitting strengths from the analytical work of Bauerheim *et al.* (2014*a*).

Results of the model fitting are displayed in Figure 8. Associated Pearson's coefficients are provided in Table 1 and are computed by the formula

$$R = \sqrt{\frac{\sum_{i=1}^{100}(\tilde{\omega}_i - \bar{\omega}_i)^2}{\sum_{i=1}^{100}(\omega_i - \bar{\omega}_i)^2}}, \tag{3.4}$$

where ω_i and $\bar{\omega}_i$ are the reference and mean growth rate from ATACAMAC and $\tilde{\omega}_i$ is the estimated growth rate using different fitting models (Figure 8). These results show that even if the weakly and strongly coupled regimes share the same active variables (Figure 7), their response surfaces (i.e., the model involving these active variables) are clearly different. For the weakly coupled mode, a linear model with the three dominant active variables is sufficient to reproduce 90% of the growth rate variations, whereas a quadratic model is required for the strongly coupled regime.

The low-order models obtained are algebraic and can be replayed efficiently at low cost. Here $100,000$ samples of these models were computed to generate the PDF of the growth rate as well as the risk factor displayed in Table 2. A good agreement is found for both regimes. The two linear models produce a higher error rate on the risk factor whereas the quadratic model is able to accurately evaluate the stability of the system: the relative risk factor error is 0.87% for the weakly coupled mode and 5% for the strongly coupled case when using this model. These results show the accuracy and efficiency of the UQ method proposed here.

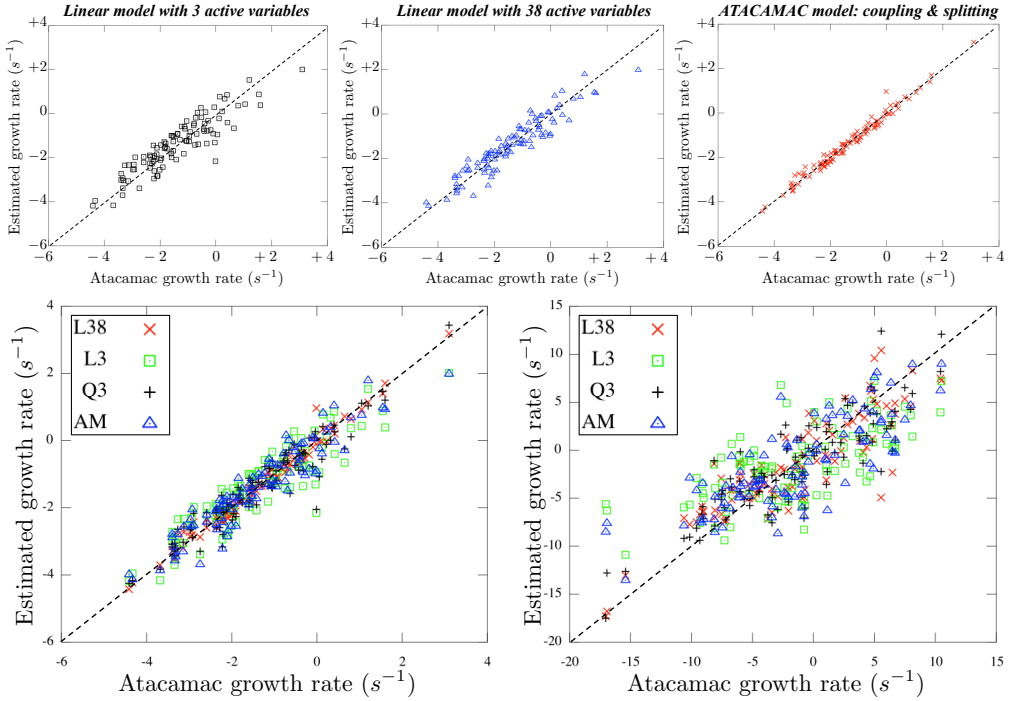

FIGURE 8. ATACAMAC growth rates (100 samples) for weakly (separate models, top, and together bottom left) and strongly (bottom right) coupled regimes are compared with estimations obtained with linear (L3 and L38), quadratic (Q3), or analytical (AM) models on all (L38), or only the three dominant active variables (L3, Q3, and AM).

4. Conclusion

For the first time, Uncertainty Quantification (UQ) has been applied to the thermo-acoustic stability of a simplified gas turbine to determine its risk factor, defined as the probability of the first azimuthal chamber mode to be unstable. The realistic configuration considered here contains an annular plenum which connects 19 burners and flames and an annular chamber which operates in two different regimes called weakly and strongly coupled regimes. Each flame is modeled by two uncertain Crocco parameters (n, τ), leading to a large UQ problem involving 38 independent parameters. A UQ method is proposed to reduce the size of the problem and is compared with a classical Monte Carlo method using the quasi-analytical ATACAMAC tool to avoid expensive Helmholtz simulations. First, the dimension of the problem is reduced from 38 to only 3 parameters using this active subspace approach based on gradient correlations. Linear and quadratic models based on the three active variables are then fit using only 100 ATACAMAC simulations. These low-order models are replayed $100,000$ times to obtain the risk factor estimation. Results show that for both regimes, the present UQ method is able to accurately predict the risk factor of the configuration with errors less that 1% for the weakly coupled case and 5% for the strongly coupled regime which demonstrates its accuracy and efficiency. This UQ method can be applied to other configuration and tools such as Helmholtz solvers instead of the ATACAMAC tool.

Acknowledgments

M. Bauerheim gratefully acknowledges support from SNECMA. Part of this study was performed wihin the UMRIDA research program (Contract No. FP7-AAT-2013-RTD-1-605036) funded by the European Community.

REFERENCES

Bauerheim, M., Cazalens, M. & Poinsot, T. 2014*a* A theoretical study of mean azimuthal flow and asymmetry effects on thermo-acoustic modes in annular combustors. *Proc. Combust. Inst.* **35**, In Press.

Bauerheim, M., Parmentier, J., Salas, P., Nicoud, F. & Poinsot, T. 2014*b* An analytical model for azimuthal thermoacoustic modes in an annular chamber fed by an annular plenum. *Combust. Flame* **161**, 1374–1389.

Constantine, P. G., Dow, E. & Wang, Q. 2014 Active subspace methods in theory and pratice: applications to kriging surfaces. *SIAM J. Sci. Stat. Comput.* **36**, 1500–1524.

Crocco, L. 1952 Aspects of combustion instability in liquid propellant rocket motors. part II. *J. American Rocket Society* **22**, 7–16.

Lieuwen, T. & Yang, V. 2005 *Combustion Instabilities in Gas Turbine Engines. Operational Experience, Fundamental Mechanisms and Modeling*, , vol. 210. Progress in Astronautics and Aeronautics, AIAA.

Nicoud, F., Benoit, L., Sensiau, C. & Poinsot, T. 2007 Acoustic modes in combustors with complex impedances and multidimensional active flames. *AIAA Journal* **45**, 426–441.

Noiray, N., Bothien, M. & Schuermans, B. 2011 Analytical and numerical analysis of staging concepts in annular gas turbines. *Combust. Theory and Modelling* **15**, 585–606.

Pankiewitz, C. & Sattelmayer, T. 2003 Time domain simulation of combustion instabilities in annular combustors. *J. Eng. Gas Turb. and Power* **125**, 677–685.

Poinsot, T. & Veynante, D. 2005 *Theoretical and Numerical Combustion*. R.T. Edwards, 2nd edition.

Polifke, W., Poncet, A., Paschereit, C. O. & Doebbeling, K. 2001 Reconstruction of acoustic transfer matrices by instationary computational fluid dynamics. *J. Sound Vib.* **245**, 483–510.

Wolf, P., Staffelbach, G., Gicquel, L., Muller, J. & T., P. 2012 Acoustic and large eddy simulation studies of azimuthal modes in annular combustion chambers. *Combust. Flame* **159**, 3398–3413.

Worth, N. & Dawson, J. 2013 Self-excited cricumferential instabilities in a model annular gas turbine combustor: global flame dynamics. *Proc. Combust. Inst.* **34**, 3127–3134.